ELSEVIER

Radiotherapy and Oncology 63 (2002) 75–81

RADIOTHERAPY & ONCOLOGY
JOURNAL OF THE EUROPEAN SOCIETY FOR THERAPEUTIC RADIOLOGY AND ONCOLOGY

www.elsevier.com/locate/radonline

An anthropomorphic phantom for quality assurance and training in gynaecological brachytherapy

Carlos Eduardo de Almeida[a,*], Miguel Rodriguez[a], Elizabeth Vianello[a], Ivaldo Humberto Ferreira[b,*], Claudio Sibata[c]

[a]*Laboratório de Ciências Radiológicas, Universidade do Estado do Rio de Janeiro (LCR-UERJ), Rio de Janeiro, Brazil*
[b]*ESTRO-EQUAL Measuring Laboratory, Service de Physique, Institut Gustave-Roussy, 39 rue Camille Desmoulins, 94805 Villejuif, France*
[c]*Radiation Oncology Department, CWRU School of Medicine, Cleveland, OH, USA*

Received 27 June 2001; received in revised form 18 February 2002; accepted 7 March 2002

Abstract

Background and purpose: An anthropomorphic water filled polymethylmethacrylate (PMMA) phantom designed to serve as a Quality Assurance (QA) tool and a training aid in brachytherapy of gynaecological tumours is investigated and presented. Several dosimetric parameters associated with the dose rate calculation can be verified with the aid of this phantom such as the source positioning, its imaging reconstruction from radiographs and the accuracy of the algorithm used for manual or computer dose rate calculation.

Material and methods: The phantom walls and the internal structure are 5 mm thick and consist of PMMA, in the form of the abdomen taken from a female Alderson Phantom Marker points representing the organs of interest were determined from computed tomography scans of a patient of similar size. Three PMMA inserts designed to hold a Farmer type ionization chamber of 0.6 cm^3 were positioned at the points to represent the bladder, rectum and point A. The formalism proposed by the IAEA TRS-277 dosimetry protocol was used for the conversion of readings of the ionization chamber to dose rate values with a modification to take into account the dose rate gradient in the detector. Five ^{137}Cs sources were used and the dose rate was evaluated by measurements and Monte Carlo simulations using the PENELOPE code. Four different treatment planning systems with different algorithms and source reconstruction techniques were also used in this investigation and compared with the manual dose rate calculations made using Karen and Breitman's tables.

Results: The dose rate calculations performed with Monte Carlo and the four treatment planning systems are in good agreement with the experimental results as well as with the manual calculations when the colpostat shielding and the tandem attenuation are taken into account. The comparison between experiment and calculations by the four treatment planning systems shows a maximum variation of 5.1% between the calculated and measured dose rate at the point A.

Conclusions: This phantom is suitable for use during the acceptance tests of treatment planning systems and applicators, as educational tool, for dosimetric research problems and for the QA of brachytherapy sources.

Keywords: Brachytherapy; Quality assurance; Training; Anthropomorphic phantom

1. Introduction

Brachytherapy is an important component of a treatment strategy for almost every stage of the gynaecological tumours.

Low dose rate ^{137}Cs tubes or spheres, and high dose rate ^{192}Ir sources inserted into different types of applicators are presently the most common sources used in gynaecological brachytherapy.

During the last few decades, considerable clinical improvements have been achieved including better follow-up of the patients, better tumour local control, less complication rates to normal tissues, design of new applicators and a better but still incomplete definition of clinical reference points recommended by the ICRU *Report* 38 [2,13]. An important contribution to this process has been the standardization of the source strength specification [17], and the availability of new calibration methods [15]. However, the existing computer programs calculate the dose rates to points or volumes ignoring the applicator heterogeneities. The concept of Quality Assurance (QA) has been introduced and it is now accepted world wide as a need to guarantee consistency and accuracy to treatment delivery [1].

Nowadays, the data gathered from new procedures specially those involving high-dose-rate (HDR) techniques are providing additional information for clinicians to exer-

* Corresponding authors.

0167-8140/02/$ - see front matter
PII: S0167-8140(02)00065-8

cise their judgement on the required dose limits associated with the overall accuracy of the entire procedure [2].

This paper describes the design and provides dosimetric data obtained with an anthropomorphic water filled Lucite (PMMA) phantom used with low dose rate ^{137}Cs sources in a Fletcher-Suit type applicator [9].

2. Materials and methods

2.1. Phantom design and specifications

A transportable anthropomorphic water filled Polymethylmethacrylate (PMMA) phantom shown in Fig. 1, was designed to hold a typical low dose rate brachytherapy applicator, in this case a Fletcher-Suit type with tungsten shielding [6,10,19].

The pelvic phantom has been modelled from a female Alderson phantom. The position of marker points representing the location of the organs of interest, bladder and rectum were determined from computed tomography (CT) scans of a patient of similar size.

The dimensions of the phantom are: 21 cm in the anterior–posterior direction (AP), 36 cm in the lateral direction (LL), and 25 cm in the axial axis. The phantom walls have a thickness of 0.5 cm and the total weight of the phantom is 400 g when empty.

The phantom dimensions are sufficient to provide full scatter conditions to ionization chamber measurements and the anthropomorphic shape simulates a real clinical situation that is important during the patient simulation.

The applicator [10] was glued to a PMMA disk in a geometry similar to a typical gynaecological treatment and was fixed to the front face of the phantom by a set of nine screws tightened on an O-ring to avoid water leakage. If a different applicator is used the PMMA disk can be replaced and the treatment geometry is maintained constant.

At the centre of those points as well as in the historical point A, ionization chamber sleeves of 1.2 mm PMMA wall thickness, made for a 0.6 cm^3 ionization chamber, were placed.

PMMA rods with lead markers simulating the dose rate calculation points of rectum, bladder and point A, are inserted into the sleeves during the acquisition of the orthogonal films, as required by the dose calculation algorithms. In this case, the markers replace the Foley balloon that gives contrast in the bladder. The contrast in the rectum and the point A are obtained directly from the X-ray images. The uncertainties involved in identifying the reference points in clinical practice were avoided by fixing the points, since the main objective is to verify the correctness of the algorithm and not the intrinsic variation from patient to patient.

2.2. Ionization chamber measurements

In order to estimate the dose rate in the reference points, five CDC-J types, ^{137}Cs (Amersham International) sources were inserted into the applicator and tandem. Two sources with linear reference with the total air kerma rate of 72.3 μGy h^{-1} m^2 cm^{-1} are inserted in the colpostats and three sources with the total air kerma rate of 54.2, 36.2 and 36.2 μGy h^{-1} m^2 cm^{-1} are inserted in the uterine tandem.

Each source strength was measured with a total uncertainty of 2.7% using a well-type ionization chamber model HDR-Plus made by Standard Imaging and previously calibrated at the Accredited Dosimetry Calibration Laboratory University of Wisconsin (ADCL-UW, USA).

A 0.6 cm^3 Farmer type ionization chamber model 2571 made by Nuclear Enterprises, with the air-kerma (N_k) factor provided for ^{137}Cs gamma rays by the ADCL-UW and a electrometer model Excalibur, made by Standard Imaging were used for the measurements. The formalism of the IAEA *TRS-277* [12] dosimetry protocol was used for the absorbed dose rate determination. This formalism was slightly modified, Eq. (1), to take into account the correction factor for the displacement of the effective point of measurement, P_d, given by Meertens [16], in this case it was taken as 0.970 and the non-uniformity of the fluence over the detector volume, P_n, as proposed by Kondo and Randolph [14].

$$D_w(P_{eff}) = M_u N_D (s_{w,air})_u p_u p_{cel} p_d p_n \quad (1)$$

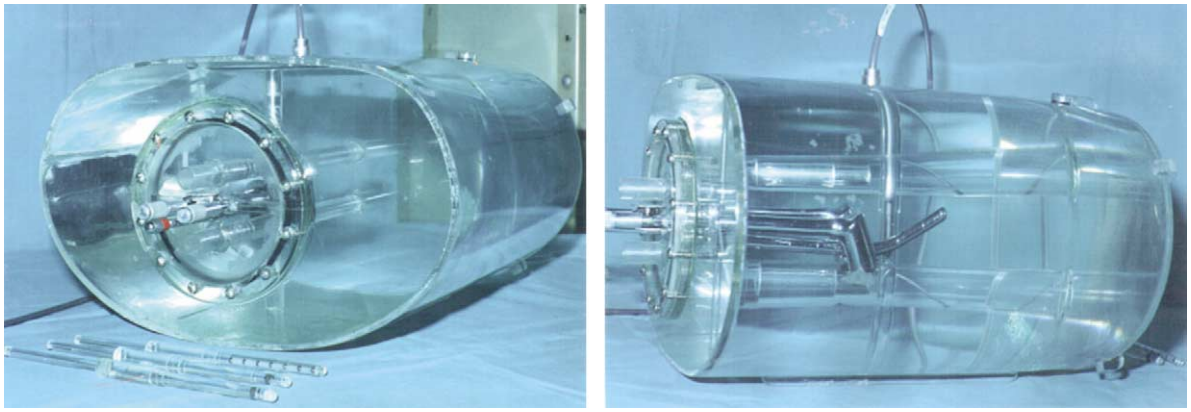

Fig. 1. (a) Water phantom with the applicator. PMMA rods with lead markers and the ionization chamber are also shown.

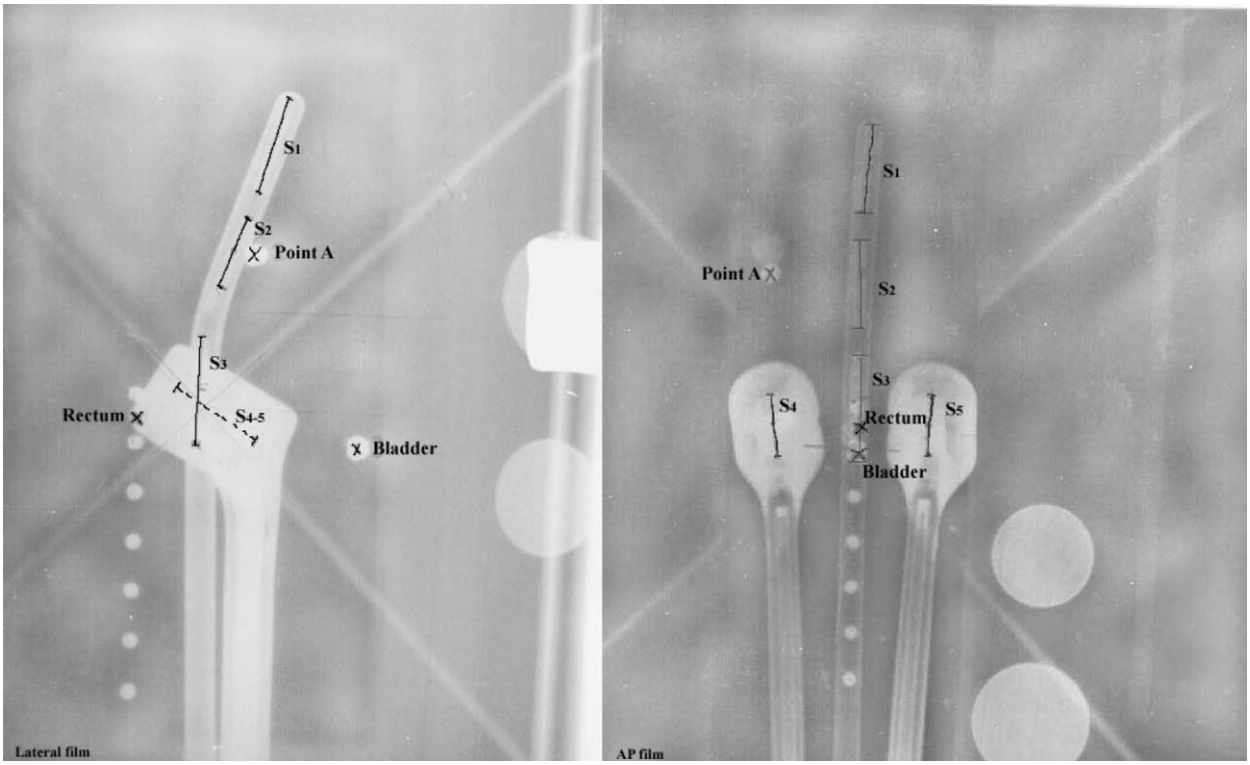

Fig. 2. The X-ray films (lateral and AP) taken of the anthropomorphic phantom filled with water, with the dummy sources and the lead markers at the reference clinical points. The total nominal activity of sources S_4 and S_5 is 72.3 Gy h^{-1} m^2 cm^{-1}, S_2 and S_3 is 36.2 Gy h^{-1} m^2 cm^{-1} and S_1 is 54.2 Gy h^{-1} m^2 cm^{-1}.

where D_w is absorbed dose to water at the point of interest (i.e. at the effective point of measurement of the chamber P_{eff}), M_u is the instrument reading, taking into account temperature, pressure, humidity, leakage, recombination and polarity, N_D is the calibration factor in terms of absorbed dose to water for ^{137}Cs, (4.3×10^7 Gy/C), $(s_{w,air})_u$ is the stopping-power ratio of water to air for ^{137}Cs, (1.136), p_u is the perturbation correction that takes into account the difference in scattering in the phantom, chamber wall and the air cavity, (1.00), p_{cel} is the correction for the non-equivalence of the centre electrode material (1.00), p_d is the correction factor for displacement of the effective point of measurement (0.970), p_n is the correction for the non-uniformity of the fluency over the detector volume taken from Kondo and Randolph, for each distance considered.

2.3. Treatment planning systems

The results of the ionization chamber measurements are compared with the dose rate calculations done using four TPS and manual calculations using the Breitman's table [4,21].

Four treatment planning systems were used for this study: the Pinnacle v3 [5] of the CWRU School of Medicine, the Theraplan v05 [20] of the LCR-UERJ, the Dosigray of the Institut Gustave-Roussy, [8] and the ISIS-C of the Institut Curie [18]. The values for the Tungsten colpostat attenuation (15.5% for rectum, 13.9% for bladder and 5.6% at the point A) found by using Monte Carlo simulations on this work have been considered on the dose rate calculations. The position and thickness of the shielding were carefully taken from X-ray images of the applicators with the appropriate magnification.

2.4. Phantom imaging

A pair of orthogonal X-rays films (Fig. 2) was taken with the phantom filled with water, the lead markers placed at the reference points and the dummy sources inside the applicator. The films were taken using a Therasim Simulator, with an AP field size of 20×25 cm^2, and a lateral field of 15×25 cm^2. This full procedure simulated with the phantom provides an educational opportunity to evaluate the correctness of the input reconstruction data, e.g. scaling factors and film quality as well as the calculation algorithm, since the exact geometry of the phantom is known. To determine the values of the fluence gradient factor P_n, the distances between each source and point of interest were calculated using the films. The values of P_n for a point source were taken from the work of Kondo and Randolph [14] and Deshpande et al [7]. In addition, the experimental values recently measured for ^{137}Cs linear sources by Vianello et al [22], were also considered in the formalism and the final results are comparable. The ionization chamber measurements were compared with the dose rate values calculated by four TPS (Theraplan v05, Pinnacle 3, ISIS-

C and Dosigray) and the manual calculations made for ^{137}Cs sources (Table 3) based on the X-ray films of the phantom.

2.5. Monte Carlo calculations

The PENELOPE Monte Carlo code was used to simulate the radiation transport in the phantom and to assess the absorbed dose rate at the clinical points. In contrast to the measurements, the Monte Carlo dose rate calculation is not affected by errors related to the positioning, energy and angular dependence of the detector and the steep dose gradients near the sources as well. The characteristics of PENELOPE code has been stated elsewhere [3], and just a brief description will be provided here. The code is implemented in FORTRAN 77 and its structure is based on a set of subroutines that are invoked from a main program written by the user. It is applicable to energies ranging from 1 keV to 1 GeV for photons and from 0.1 keV to 1 GeV for electrons. The code simulates incoherent scattering, coherent scattering and Bremsstrahlung X-ray production. The electron binding effects and Doppler broadening are taken into account for incoherent scattering. In addition, characteristic k-shell X-rays and Auger electrons' emission following photoelectric absorption is also simulated. Electron and positron histories are generated on the basis of a mixed algorithm that combines detailed simulation of hard events with condensed simulation of soft events. The package for geometry definition is based on the combination of surfaces (represented by quadratics functions) to form the more complex structures such as bodies and body sets (modules).

2.5.1. Sources and phantom geometry

The CDC-J ^{137}Cs source is a cylindrical source of 0.265 cm in diameter and 2 cm in length. The active material is distributed in an internal cylinder of 0.165 cm in diameter and 1.35 cm in length and consists of Cesium bound with a low attenuation ion exchange medium of zirconium phosphate with a density of 1.63 g cm^{-3}. The source encapsulation material is composed of 80% platinum and 20% iridium [15]. The source was modelled with PENELOPE as a pair of concentric cylinders with materials and dimensions as described previously.

The phantom shape and its internal structure were also modelled with PENELOPE and the phantom was considered as filled with liquid water (density of 1 g cm^{-3}). PMMA phantom walls were not modelled since their presence does not have any influence in the dose rate calculated at the reference points.

The internal structure of the Fletcher-Suit applicator inserted into the phantom is shown in Fig. 3. The colpostat has a stainless steel body, shaped as a cylinder of 2 cm in diameter and 3 cm in length and a wall thickness of 0.5 cm with an internal cavity to hold the source. The Tungsten shields of 0.5 cm thickness are located in the superior and inferior extremes. The effective top section of the colpostat shields is defined from 35 to 160° and the bottom section from 45 to 225°, as shown in Fig. 3. The uterine tandem is

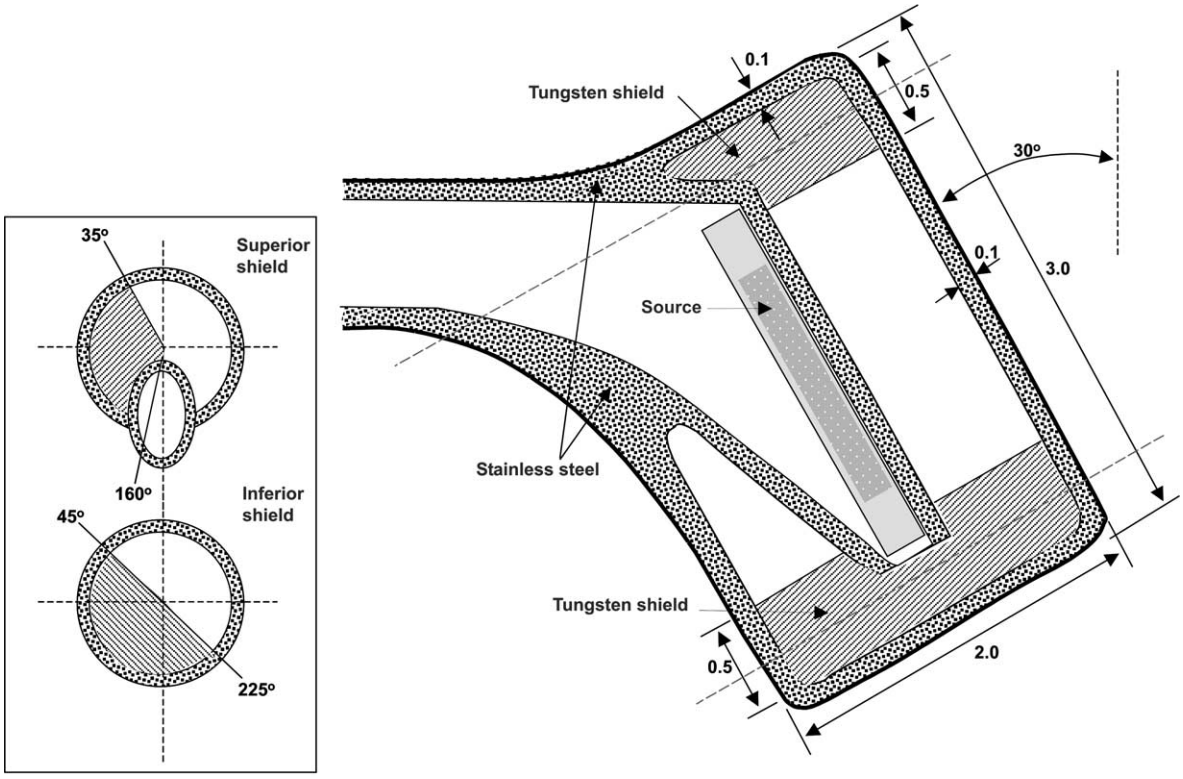

Fig. 3. Diagram shows the dimensions of the colpostat applicator. Insert shows a top view of the stainless steel walls with the position of the tungsten shields.

Table 1
Positions of the markers' points in the phantom relative to the coordinate system as described in the text

Site	X (cm)	Y (cm)	Z (cm)
Point A	− 2.1	3.75	0.5
Rectum	0.0	0.0	− 1.5
Bladder	0.0	− 0.4	3.1

made of stainless steel with an external diameter of 0.6 cm and a wall thickness of 0.5 cm. The complex 15° curvature of the tandem was simulated by a series of short cylinders rotating in increasing angles. The Cartesian coordinate system for the phantom simulation was positioned as follows: X from left to right, Y from top to bottom (along the applicator) and Z from front to back; the origin is located at the centre of the colpostats in the plane $X = 0$ and the half-distance between both colpostats in the plane $Z = 0$. The positions of the clinical points in this system of coordinates are shown in Table 1.As many as 125 surfaces and 50 bodies were needed to accurately reconstruct the phantom and the sources geometry as described previously.

2.5.2. Dose rate calculation

For the dose rate calculation using the PENELOPE code, charged particle equilibrium was assumed to exist [23], allowing the absorbed dose rate to be approximated by collision kerma. The contribution to the dose rate from electrons produced in the colpostats or tandem structure was not considered. The exponential track-length estimator [3,6,7] was used to calculate the collision kerma. For this purpose, a subroutine named TRLEN was written in FORTRAN 77 which perform ray-tracing along the photon trajectory between collisions. The photon contribution to collision kerma was estimated in a set of spherical scoring volumes whose locations and dimensions are considered in the subroutine as input parameters. Scoring volumes radii from 0.1 to 0.15 cm were used for the average source-point distances ranging from 1.5 to 3.75 cm as recommended by Williamson [24,25]. The photon linear attenuation and mass energy-absorption coefficients were taken from Hubbell and Seltzer [11].

A configuration of five sources with geometry and air kerma strength as previously described was simulated. The positions of the sources placed into the tandem were estimated from measurements done in a lateral X-ray film of the phantom with the applicator loaded with dummy sources.

In order to evaluate the applicator influence in the absorbed dose rate at the studied points, two configurations of the phantom geometry were considered: one including the applicator and tandem filled with the sources, and a second including just the sources, arranged in the same way as if they were inside the applicator and tandem. For each configuration, a set of five simulations with a total of 2×10^8 photon histories each was performed.

3. Results and discussion

3.1. Ionization chamber measurements

The results of the dose rate measured at the clinically relevant points with the ionization chamber are shown in Table 3. Systematic differences are observed between the measured values with the ionization chamber and the values calculated by all treatment planning systems since the latter ignore the presence of the applicator and its shielding.

3.2. Monte Carlo simulation

The results of the Monte Carlo simulations are presented in Table 2, which contains the calculated dose rate for the clinical points performed for the two phantom configurations simulated. These results indicate that the effect of the applicator shielding reduces the dose rate to the rectum, the bladder and point A by 18.4, 16.3 and 5.9%, respectively.

The standard deviations shown in Table 2 correspond to the standard error of the mean obtained in the estimation of the dose rate by the Monte Carlo code, being in all cases less than 1%. Table 2 further breaks down the total attenuation in attenuation due to the applicator walls and the rectum and bladder shields.

3.3. Comparison of the results

The dose rate calculated by the Monte Carlo method at the clinical points defined in the phantom with the applicator and tandem agrees well with the experimental results. The relative differences between these values are 0.98, 0.79 and 0.98% for rectum, bladder and Point A, respectively, and are well within the uncertainties of the measurements. In

Table 2
Results of the calculated dose rate by the Monte Carlo method at the markers' points with and without the applicator

Site	Dose rate (cGy h^{-1})			
	Sources only ($\pm 1\sigma$)	Applicator ($\pm 1\sigma$)	Dose rate reduction due to applicator wall and shielding (%)	Dose rate reduction due to the shielding only (%)
Point A	46.29 ± 0.40	43.71 ± 0.36	5.9	–
Rectum	92.89 ± 0.73	78.43 ± 0.40	18.4	11.4
Bladder	33.76 ± 0.31	29.04 ± 0.24	16.3	9.4

Table 3
Comparison of the calculated dose rates obtained with the treatment planning systems (Pinnacle, Theraplan, Dosigray, and ISIS-C), Monte Carlo and manual calculations and the ionization chamber measurements[a]

Clinical Points	Pinnacle	Theraplan	Dosigray	ISIS	Monte Carlo Sources only	Manual Calculations	Measurements
Bladder	33.24 (0.8%)	33.90 (1.2%)	34.20 (2.1%)	34.10 (1.8%)	33.76 (−0.8%)	33.92 (1.3%)	28.81
Rectum	94.24 (0.5%)	95.40 (1.7%)	96.30 (2.7%)	96.00 (2.3%)	92.89 (−1.0%)	93.65 (−0.2)	79.20
Point A	44.48 (−5.1%)	44.70 (−4.6%)	45.90 (−1.8%)	45.0 (−3.9%)	46.29 (−1.0%)	45.83 (−2.0%)	44.14

[a] The dose rate values are in cGy h^{-1}. The values in parenthesis are the differences in percent between the measured and the dose rate calculations taking into account the applicator and colpostat shielding attenuation.

contrast to the Monte Carlo calculations the chamber measurements are subject to higher uncertainties due to the high dose rate gradients inside its cavity. Slight differences between the effective point of measurement of the chamber and the location of the small scoring volumes used for dose rate calculation in Monte Carlo, may be responsible for part of the differences found. The modified formalism employed for dose rate calculation have incorporated corrections for those phenomena based on theoretical approximations. On the other hand, the dose rate calculation made by Monte Carlo is based on the approximation that electronic equilibrium exists and the photon fluence is estimated from an approximated model.

The relative differences between both sets of results suggest that any of them may be used as reference value, especially when the results are obtained from further attempts to estimate the dose rate at these points by less accurate methods.

Table 3 summarizes the calculation done with four commercial treatment planning systems, Monte Carlo and manual calculations and the experimental measurements. All calculations were done with no attenuation due to the applicator walls or the shields. A comparison of the attenuated dose rate with the measurements shows a maximum of 5.1% difference between the dose rate at the point A and the measurement at this point. All treatment planning systems, with the exception of one (Dosigray) had larger differences between the calculation and measurements made at the Point A when the attenuation of the applicator wall and shields were taken into account. Since the input of points and sources were made using the digitization of points from a pair of orthogonal films, the position of the points and the sources are highly dependent on how the digitization was done. This may account for the variation between the different planning systems and with the measurements. The calculation and measurement for the bladder and rectum are in better agreement. They are further away from the sources and a small change in their position does not translate in larger dose rate variation.

4. Conclusions

Anthropomorphic water filled PMMA phantom was designed and tested for QA in gynaecological brachytherapy. Its anatomical shape gives a closer sense of the real patient situation, since the phantom imaging and reconstruction techniques can be more realistically simulated.

The results of this work provide dose rate calculation at various clinical reference points of the anthropomorphic phantom with sufficient accuracy to be used as reference values. This allows this phantom to become a useful tool in QA, dedicated to assess the correctness of the treatment dose delivered in brachytherapy by evaluating the accuracy of the algorithms involving the dose rate calculation and image reconstruction, implemented in a Treatment Planning System.

This phantom may also play an important role in the training of the residents in radiation oncology and medical physics involved in the brachytherapy treatment.

Acknowledgements

The authors wish to thank Dr Carlos M. de Araujo and Dr Célia Viegas for supporting the part of this work done at the Instituto Nacional de Câncer. This work was partially sponsored by Grants from the FAPERJ and IAEA.

We wish to thank G. Boisserie (Hôpital Pitié-salpêtrière, Paris, France) and Dr E. Briot (Institut Gustave-Roussy, Villejuif, France) for providing the ISIS-C and Dosigray Treatment Planning Systems for this study.

References

[1] AAPM (American Association of Physicists in Medicine). Report Task Group 40. Comprehensive QA for Radiation Oncology. Med Phys 1994;21:581.
[2] de Almeida CE, Almond PR. The ICRU 38, a need for a new edition. Radiother Oncol 1997;42:315–316.
[3] Baró J, Sempau J, Fernández-Varea JM, Salvat F. PENELOPE: an algorithm for Monte Carlo simulation of the penetration and energy loss of electrons and positrons in matter. Nucl Instrum Methods 1995;B100:31–46.
[4] Breitman KE. Dose-rate tables for clinical ^{137}Cs sources sheathed in platinum. Br J Radiol 1974;47:657–664.
[5] Cassel KJ. A fundamental approach to the design of a dose-rate calculation program for use in brachytherapy. Br J Radiol 1983;56:113–119.
[6] Delclos L, Fletcher G, Sampiere V. Can the Fletcher Gamma Ray colpostat system be extrapolated to other systems? Cancer 1978;41(3):970–979.
[7] Deshpande DD, Pradhan AS, Avadhani JS, Viswanathn PS. Measure-

ment of air kerma rate and absorbed dose for brachytherapy sources with secondary standard dosimeter. J Med Phys 1996;21(4):196–201.
[8] Dosigray – TPS User's manual. Villejuif, France: Institut Gustave-Roussy (IGR), 1995.
[9] Fletcher G. Cervical radium applicators with screening in the direction of the bladder and rectum. Radiology 1953;60:77–84.
[10] Green A, Broadwater J, Hancock J. Afterloading vaginal ovoids. Am J Roentgenol 1969;105:609–613.
[11] Hubbell JH, Seltzer SM. Tables of X-ray mass attenuation coefficients and mass energy-absorption coefficients (version 1.03), [Online]. Available: http://physics.nist.gov/ xaamdi [2001, July 18]. National Institute of Standards and Technology, Gaithersburg, MD, 1997.
[12] IAEA (International Atomic Energy Agency). Absorbed dose determination in photon and electron beams: an international code of practice. IAEA, Technical Reports Series 277. 2nd ed. Vienna: IAEA, 1997.
[13] ICRU (International Commission on Radiation Units and Measurements). Dose and volume specification for reporting intracavitary therapy in gynecology. ICRU Report No 38. Bethesda, MD: ICRU, 1985.
[14] Kondo S, Randolph ML. Effects of finite size of ionization chambers on measurements of small photon sources from electrons arising in the wall of an ionization chamber. Radiat Res 1960;13:37–60.
[15] Marechal MH, Sibata CH, de Almeida CE. A calibration method for high dose rate Ir-192 brachytherapy sources. IAEA TECDOC – 896. Vienna: IAEA, 1996. p. 203–6.
[16] Meertens H. In phantom calibration of selectron-LDR sources. Quality assurance in brachytherapy. Radiother Oncol 1990;17:369–378.
[17] Nath R. Source strength specification, calibration, and dosimetric characteristics of brachytherapy sources and the ICWG dose calculation formalism for interstitial brachytherapy. In: James Purdy, editor. Advances in radiation oncology physics AAPM monograph # 19, 1990.
[18] Rosenwald JC. Automatic localization of curved wires used in brachytherapy – the COUREP program. Comput Programs Biomed 1975:103–112.
[19] Stitt J, Dean RD, Mansfield CM. Dosimetric comparison of the fletcher family of gynaecological colpostats. Int J Radiat Oncol Biol Phys 1980;11:1317–1321.
[20] Theratronics, IL, TP-11. Theraplan user's manual. Ontario: Canada, 1990.
[21] Vianello E, Biaggio M, de Almeida CE. Método manual de cálculo de dose em braquiterapia (in portuguese). Radiologia Brasileira 1998;31:285–288.
[22] Vianello E, De Biaggio MF, de Almeida CE. Experimental validation of the theraplan/TP 11(Vo5) for gynaecological treatments. Proceedings of the World Congress on Medical Physics and Biomedical Engineering, NICE IOMP 1997, September 1997. p. 850.
[23] Williamson JF, Seminoff T. Template-guided interstitial implants: Cs-137 reusable sources as a substitute for 192-Ir. Radiology 1987;165:265–269.
[24] Williamson JF, Li Z. Monte Carlo aided dosimetry of the microselectron pulsed and high dose-rate ^{192}Ir sources. Med Phys 1995;22:809–819.
[25] Williamson JF. Monte Carlo evaluation of kerma at a point for photon transport problems. Med Phys 1987;14(4):567–576.